How to cite: *Angew. Chem. Int. Ed.* **2023**, *62*, e202311186
doi.org/10.1002/anie.202311186

Peptide Modification | Hot Paper

Merging the Isonitrile-Tetrazine (4+1) Cycloaddition and the Ugi Four-Component Reaction into a Single Multicomponent Process

Yanira Méndez, Aldrin V. Vasco, Galway Ivey, Ana Laura Dias, Peter Gierth, Bárbara B. Sousa, Claudio D. Navo, Angel Torres-Mozas, Tiago Rodrigues, Gonzalo Jiménez-Osés, and Gonçalo J. L. Bernardes**

Abstract: Multicomponent reactions are of utmost importance at generating a unique, wide, and complex chemical space. Herein we describe a novel multicomponent approach based on the combination of the isonitrile-tetrazine (4+1) cycloaddition and the Ugi four-component reaction to generate pyrazole amide derivatives. The scope of the reaction as well as mechanistic insights governing the 4*H*-pyrazol-4-imine tautomerization are provided. This multicomponent process provides access to a new chemical space of pyrazole amide derivatives and offers a tool for peptide modification and stapling.

The versatility of isonitriles when reacting with strong electrophiles and nucleophiles or undergoing their simultaneous addition makes them a powerful tool for organic chemists.[1] Isonitrile-based multicomponent reactions (iMCRs),[2] since pioneering research by Passerini[3] and Ugi,[4] have changed the perception of molecular diversity and complexity towards the discovery of a wider chemical space.[5]

The Ugi four-component reaction (Ugi-4CR) involves the condensation of a primary amine, an aldehyde, a carboxylic acid and an isonitrile to afford an α-aminoacyl amide. The variation of the original set of components has generated dissimilar Ugi-type MCRs like the Ugi-Joullié MCR,[6] where a cyclic imine generated in situ replaces the amine and aldehyde components. Nevertheless, the discovery of new iMCRs is far from satisfying the growing demand of new diversity-oriented processes.[7]

Isonitriles and 1,2,4,5-tetrazines undergo a fast inverse electron demand (4+1) cycloaddition to yield a 4*H*-pyrazol-4-imine upon N_2 release. Primary isonitriles afford 4*H*-pyrazol-4-imines that undergo rapid tautomerization to aromatic pyrazole imines (Scheme 1).[8] The hydrolysis of the later imine generates a pyrazole amine and an aldehyde,

[*] Dr. Y. Méndez, Dr. A. V. Vasco, G. Ivey, Dr. P. Gierth, Prof. G. J. L. Bernardes
Yusuf Hamied Department of Chemistry, University of Cambridge
Lensfield Road, Cambridge CB2 1EW (UK)
E-mail: ym394@cam.ac.uk
gb453@cam.ac.uk

B. B. Sousa, Prof. G. J. L. Bernardes
Instituto de Medicina Molecular João Lobo Antunes, Faculdade de Medicina Universidade de Lisboa
Avenida Professor Egas Moniz, 1649-028 Lisboa (Portugal)

A. L. Dias, Dr. T. Rodrigues
Research Institute for Medicines (iMed), Faculty of Pharmacy, University of Lisbon
Av. Prof Gama Pinto, 1649-003 Lisbon (Portugal)

Dr. C. D. Navo, A. Torres-Mozas, Dr. G. Jiménez-Osés
Center for Cooperative Research in Biosciences (CIC bioGUNE), Basque Research and Technology Alliance (BRTA)
Bizkaia Technology Park, Building 800, 48160 Derio (Spain)

Dr. G. Jiménez-Osés
Ikerbaske, Basque Foundation for Science
48013 Bilbao (Spain)

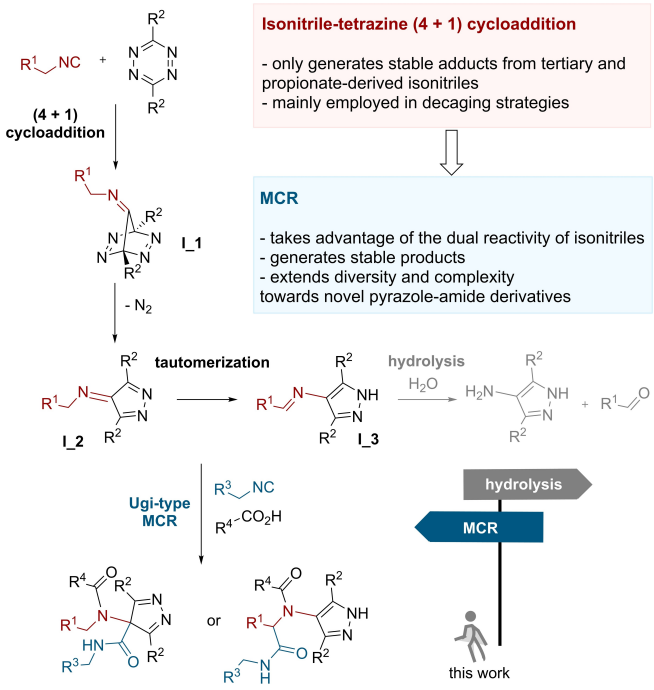

Scheme 1. Merging of isonitrile-tetrazine (4+1) cycloaddition and Ugi-4CR into a multicomponent process.

which has been exploited at decaging isocyanoalkyl-derived probes.[9]

Stable adducts are only formed when tertiary and propionate-derived isonitriles are employed,[10] or when the intermediate pyrazole imine is later reduced.[11]

A closer look at both the 4*H*-pyrazol-4-imine **I_2** and its corresponding aromatic tautomer **I_3** suggests that their reactivity could be brought into play by expanding isonitrile chemistry (Scheme 1). The participation of a second equivalent of the isonitrile and a carboxylic acid, could lead to an iMCR, where the isonitrile will have two different roles: to provide a reactive imine and to react in an Ugi-type MCR, thus closing the cycle by generating a stable product.

Herein we report the discovery of a multicomponent reaction involving a 1,2,4,5-tetrazine, two isonitriles, and a carboxylic acid to yield a pyrazole amide derivative. We hypothesized that two setups were possible, an all-in-one approach involving two equivalents of the same isonitrile, or a stepwise approach involving two different isonitriles and therefore leading to a higher chemical complexity in one pot.

To investigate the reactivity of the two intermediate imines, a series of experiments were designed in which the reaction of 3,6-di(pyridin-2-yl)-1,2,4,5-tetrazine (dPyTz) with *n*-butyl isonitrile (*n*-bNC) (1.2 equiv) was followed by the addition of acetic acid (1.2 equiv) and 1.2 extra equivalents of the isonitrile. The stepwise reaction was performed in dry dichloromethane (60.5 mmol/L) at room temperature (Table 1, entry 1). The disappearance of the starting materials in the first step was evidenced by the color change from bright fuchsia – characteristic of this tetrazine – to light yellow, in approximately 80 min. When acetic acid and a second equivalent of *n*-bNC were added, an immediate color change to dark orange and the appearance of a precipitate were noticed (Figure S1). Adding a few drops of trifluoroethanol (TFE) right after the second equivalent of isonitrile helped to solubilize the reaction product. The reaction was followed by LC-MS, and conversion towards the final condensation product was completed in around 40 min. ^{1}H NMR spectroscopy enabled the identification of a product arising from the aromatic pyrazole **I_3**, characterized by a broad singlet at 12.05 ppm and a doublet of doublets at 4.56 ppm (Figure S47). This product (**1**), in which a stereogenic center is created after reaction with a second equivalent of isonitrile and acetic acid, was isolated as a racemic mixture. To explore the possibility of a reaction occurring from **I_2** instead, the first reaction step was allowed to occur for only 20 min, and alternatively, in situ (Table 1, entry 2). However, all NMR spectra matched to a unique structure (Figure S50).

To better understand the bias towards a single product, the reaction between dPyTz (0.042 mmol) and *n*-bNC (0.055 mmol) was monitored by ^{1}H NMR spectroscopy. The reaction was performed in dry $CDCl_3$ (0.7 mL) at 25 °C, and a ^{1}H NMR spectrum was measured every 20 s for 4 h (Figure 1). From $t=1$ min, a signal at around 2.5 ppm (Figure 1, green arrow), corresponding to the alpha methylene group of **I_3**, was observed. A detailed analysis facilitated identification of the rest of the signals of this intermediate, which proportionally increase over time. While no signal belonging to **I_2** was observed at any point, a signal belonging to the hydrolysis product from **I_3** (butyraldehyde) was observed after 20 min, owing to the presence of water traces in the environment.

Tetrazines with substituents other than 2-pyridyl required longer reaction times for complete conversion. While

Table 1: Different tetrazines and their MCRs with *n*-bNC and acetic acid.

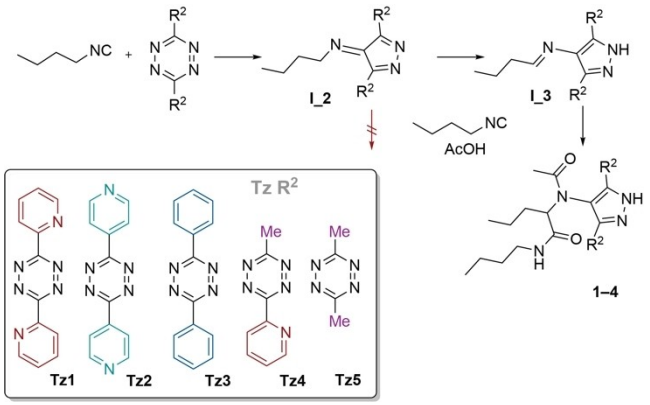

Entry	Product	Tz	Strategy[a]	Time	Yield [%]
1	**1**	**1**	a	110 min	61
2	**1**	**1**	b	90 min	44
3	–	**2**	a	110 min	NP
4	**2**	**3**	a	68 h	81
5	**3**	**4**	a	260 min	63
6	**4**	**5**	a	66 h	36

[a] Strategy a: stepwise; strategy b: in situ. NP: no product.

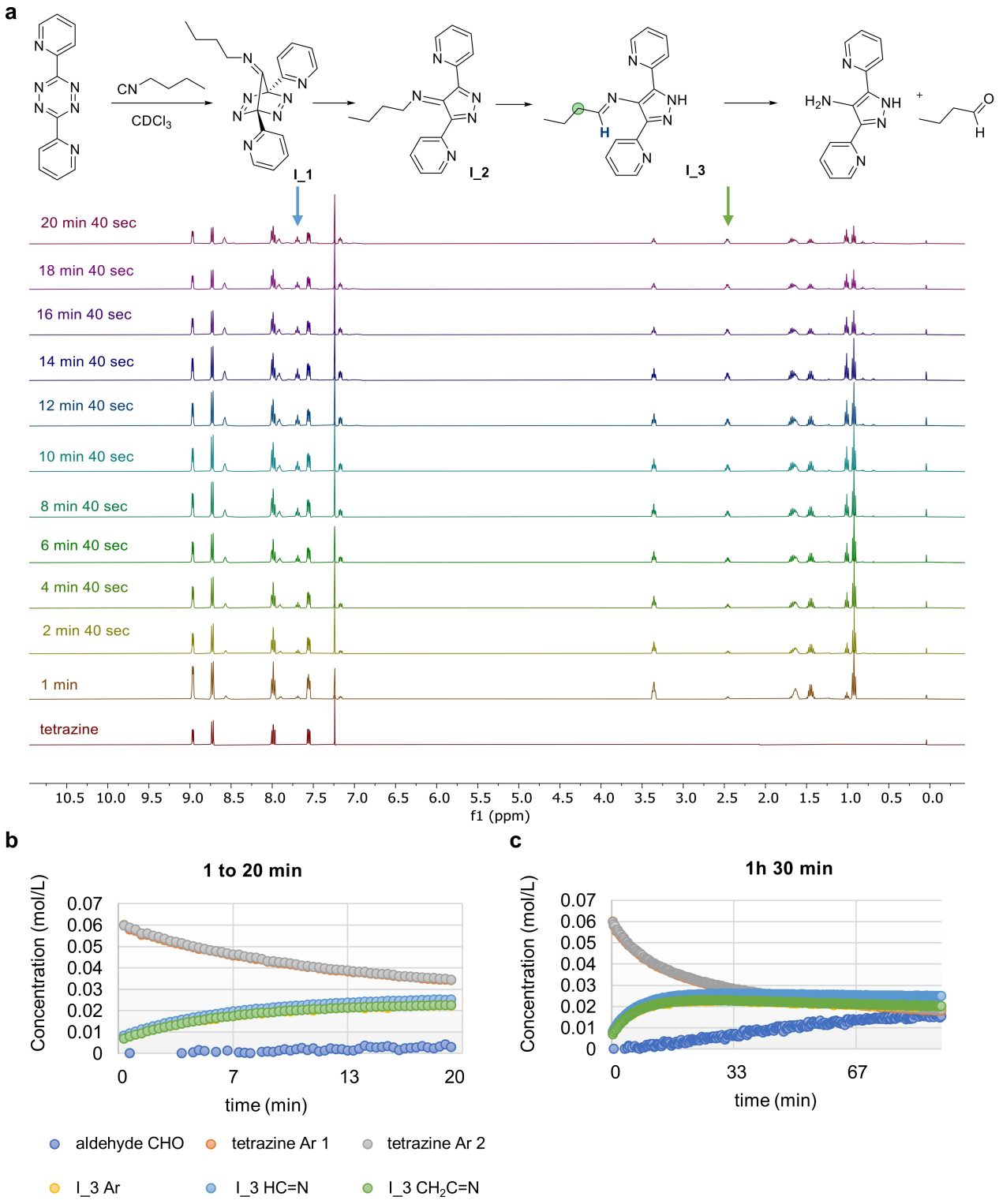

Figure 1. a) ^{1}H NMR monitoring of the reaction between *n*-bNC and dPyTz in $CDCl_3$. b, c) dPyTz concentration decay ($\delta = 8.74$; 8.98 ppm), and **I_3** ($\delta = 2.47$; 7.69; 7.90 ppm) and butyraldehyde ($\delta = 9.73$ ppm) concentration increase after b) 20 min and c) 90 min.

no product was observed for 3,6-di(pyridin-4-yl)-1,2,4,5-tetrazine (**Tz2**)—of known reduced stability[12]—(Table 1, entry 3), the reactions involving dimethyl and diphenyl tetrazines required around 66 h to reach completion (Table 1, entries 4 and 6). Further ^{1}H NMR studies of the reaction step involving 3,6-diphenyl-1,2,4,5-tetrazine (dPhTz) and *n*-bNC (see the Supporting Information) showed that **I_2** was rather stable for the first 5 h (ca. 23 %) and that only after 14 h a reasonable amount of **I_3** (ca. 30 %) accumulated, which explains the poorer reaction

kinetics. This also suggests that the 2-pyridyl nitrogen atom may assist the hydrogen transfer in the tautomerization process from **I_2** to **I_3**.

A DFT study was performed to analyze the influence of the pyridyl and phenyl groups on both the cycloaddition reaction between abbreviated models of the reactants (*n*-bNC and dPyTz or dPhTz) and the subsequent tautomerization step from adducts **I_2** to **I_3** in aprotic solvents (i.e. chloroform). The [4+2] cheletropic cycloaddition reaction between isocyanoethane (EtNC) and dPyTz was calculated to be more favored (**TScyc_Py**, $\Delta G^{\ddagger} = 24.1$ kcal mol^{-1}) than with dPhTz (**TScyc_Ph**, $\Delta G^{\ddagger} = 26.8$ kcal mol^{-1}) owing to the higher electron-withdrawing character of pyridine (Figure 2). These results agree with the faster kinetics observed for dPyTz as compared to dPhTz. Regarding the tautomerization process, the nitrogen atom of the pyridine group in intermediate **I_2_Py** may act as a base to assist C–H deprotonation (**Py_TS1**, $\Delta G^{\ddagger} = 21.6$ kcal mol^{-1}) and form a pyridinium zwitterion **I_2b_Py** ($\Delta G = -22.0$ kcal mol^{-1}), which is in a fast equilibrium with a slightly more stable iminium zwitterion **I_2c_Py** (Figures 3a and S72).

Finally, the most stable **I_3_Py** intermediate ($\Delta G = -35.3$ kcal mol^{-1}) is obtained from **I_2b_Py** upon very fast and highly exergonic hydrogen atom transfer (HAT) from the pyridinium group to the pyrazole group after rotation of one pyridine ring (Figure S72).

Hence, the 2-pyridyl substituents of the tetrazine would play a key dual role (i.e. base and proton shuttle) to promote intramolecular tautomerization.

An analogous tautomerization process by intramolecular HAT is not possible for **I_2_Ph** and, hence, different mechanistic possibilities have been considered. First, the intramolecular 1,2-proton shift from **I_2_Ph** to form an iminium zwitterion intermediate **I_2c_Ph** was calculated to have a prohibitive activation barrier (**Py_TS1**, $\Delta G^{\ddagger} = 43.1$ kcal mol^{-1}) due to the inefficient overlap of the orbitals involved in the process (Figure 3b). Introducing one to three water molecules (assumed to be present as solvent traces) as a proton shuttle relaxes and stabilizes the proton shift transition structure, which significantly and gradually lowers the activation barrier ($\Delta G^{\ddagger}$ from 34.6 to 25.4 kcal mol^{-1}; Figure 3c). Of note, the direct 1,5-proton shift to **I_3_Ph** was calculated to be facilitated also by a cluster of three water molecules, with a lower activation barrier (**TS2_Ph_3xH$_2$O**, $\Delta G^{\ddagger} = 22.7$ kcal mol^{-1}). Nevertheless, even the most favoured water-assisted tautomerizations from **I_2_Ph** show activation barriers slightly higher than that calculated from **I_2b_Py** ($\Delta\Delta G^{\ddagger} \approx 1$–4 kcal mol^{-1} depending on the mechanism and/or amount of water traces). This trend agrees with the experimental outcome that the reaction with the dipyridyl derivative rapidly forms intermediate **I_3_Py** even in aprotic media, while formation of diphenyl intermediate **I_3_Ph** is much slower.

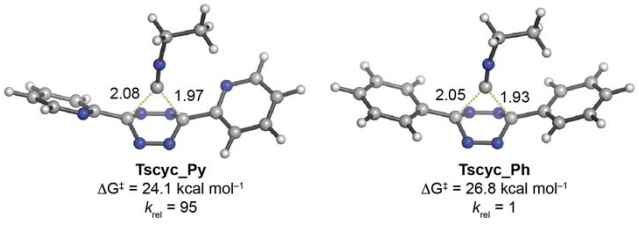

Figure 2. Geometries, relative activation energies ($\Delta G^{\ddagger}$) and relative reaction rate constants at 25 °C (k_{rel}) for the cycloaddition reaction between dPhTz and dPyTz with EtNC calculated with PCM($CHCl_3$)/M06-2X/6-31+G(d,p). Forming bonds are shown as green dashed lines. Distances are given in angstrom.

In a subsequent experiment conducted in a stepwise manner, 10 % pyridine was added to the reaction of dPhTz (0.085 mmol), *n*-bNC (0.170 mmol) and acetic acid (0.085 mmol). In agreement with our predictions, the presence of substoichiometric amounts of pyridine accelerates the formation of the pyrazole amide product and precludes the accumulation of intermediates, demonstrating its role as a proton shuttle for the necessary tautomerization step (Figure S70).

Thereafter, the possibility of MCRs involving secondary and tertiary isonitriles was explored with cyclohexyl and *tert*-butyl isonitriles (Table 2, entries 1 and 2). The reaction of *tert*-butyl isonitrile with tetrazines affords stable 4*H*-pyrazol-4-imines owing to the abrogation of the tautomerization step. In both cases, an MCR involving acetic acid and a second equivalent of the same or a different isonitrile did not occur, probably owing to the formation of secondary intermediate imines (**I_2**), which are known to be less reactive in Ugi-type MCRs. This corroborates the results from the MCRs involving primary isonitriles, taking place only from the aromatic pyrazole imines **I_3**.

To demonstrate the feasibility of combining different isonitriles, two setups were explored, where *n*-bNC was employed in the first step and either cyclohexyl isonitrile (Table 2, entry 3) or *tert*-butyl isonitrile (Table 2, entry 4) was employed in the second step. Both reactions proved efficient at affording the expected products in 71 and 67 % yield, respectively. With these results in hand, the reaction scope for different carboxylic acids was also investigated. Using longer carboxylic acids, such as 2-(2-(2-methoxyethoxy)ethoxy)acetic acid (Table 2, entry 5) and myristic acid (Table 2, entry 6) also proved efficient, and in both cases the in situ reactions in DCM/TFE/H_2O afforded higher yields (see the Supporting Information). Combining different hydrophilic tetrazines and isonitriles in either TFE or aqueous solvents also proved efficient (Table 2, entries 7 and 8). However, the use of aqueous systems did also favor the hydrolysis of the corresponding imine intermediates, thus substantially reducing the reaction yields.

Extending the reaction scope to more complex substrates, such as peptides, was explored. For this purpose, the pentapeptide Lys-Cys(S-*t*Bu)-Gly-Ser-Phe was assembled on a TentaGel S-RAM resin. After removing the S-*t*Bu protecting group, the Michael addition of the cysteine sulfhydryl group to two bifunctional maleimides, one containing a primary isonitrile and the other a phenyl methyl tetrazine, was performed. *n*-bNC, dPyTz and either acetic acid or *d*-desthiobiotin were selected as the soluble components of the MCR.

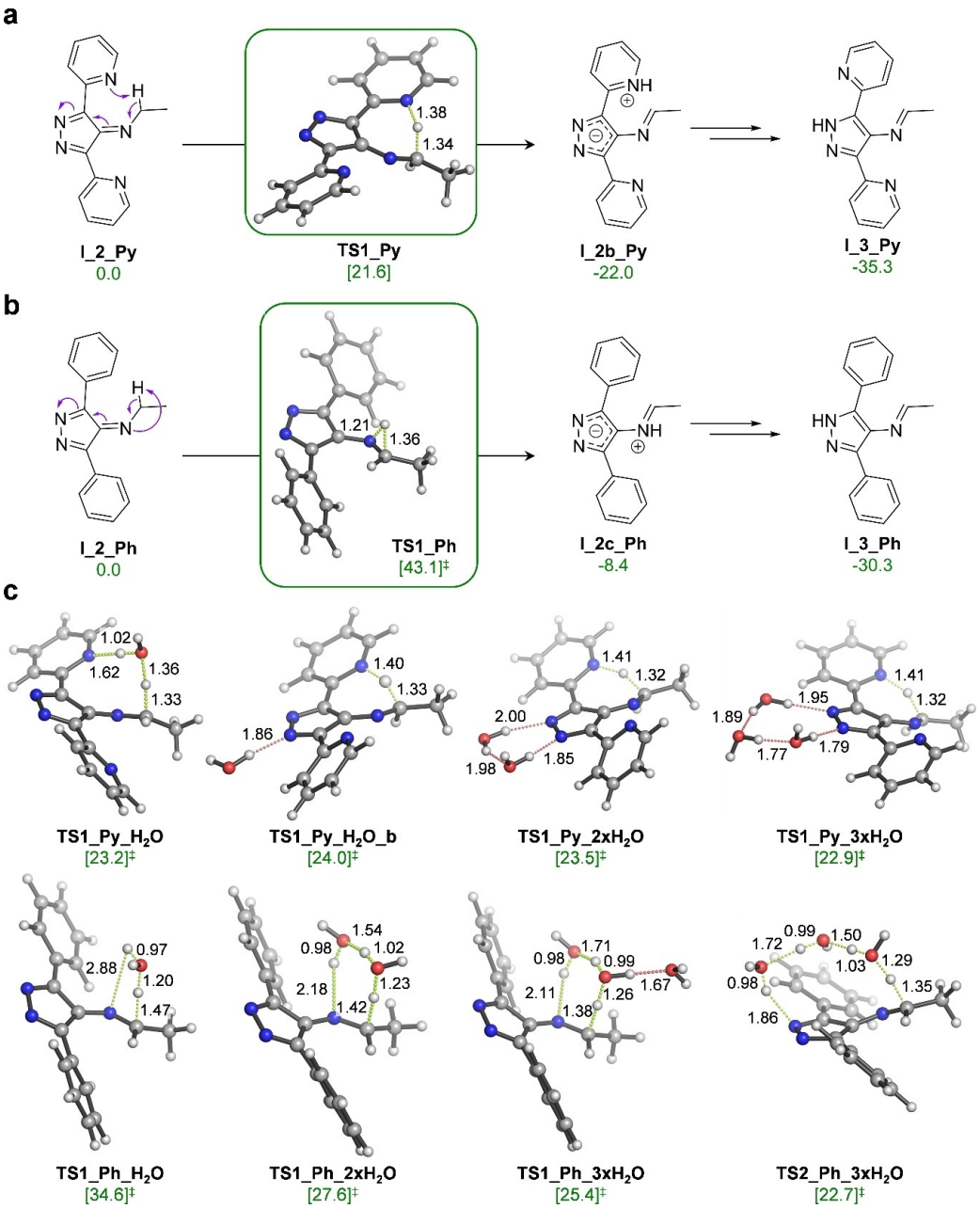

Figure 3. a) Intramolecular pyridine-assisted tautomerization from **I_2_Py** to afford **I_3_Py**. b) Intramolecular 1,2-proton shift from **I_2_Ph** to form iminium zwitterion intermediate **I_2c_Ph** and subsequently **I_3_Ph**. c) Water-assisted deprotonation (**TS1_Py_*n*xH$_2$O** to form **I_2b_Ph**), 1,2-H shift (**TS1_Ph_*n*xH$_2$O** to form **I_2c_Ph**) and 1,5-H shift (**TS2_Ph_3xH$_2$O** to form **I_3_Ph**) catalyzed by 1–3 water molecules ($n=1$–3). Geometries and relative energies (ΔG and $\Delta G^{\ddagger}$, given in kcal mol^{-1}) were calculated with PCM($CHCl_3$)/M06-2X/6-31+G(d,p). Breaking/forming bonds at the transition structures are shown as green dashed lines. Hydrogen bonds are shown as red dashed lines. Distances are given in angstrom.

The tetrazine-modified peptide was allowed to react in situ with a 5-fold excess of the carboxylic acid and a 10-fold excess of *n*-bNC. On the other hand, the isonitrile-modified peptide was first treated with a 5-fold excess of the carboxylic acid and then a 5-fold excess of a preincubated mixture of *n*-bNC and dPyTz (10 min incubation). The reason behind the later setup was to avoid the parallel formation of two different pyrazole imines from the immobilized/soluble isonitriles. As shown in Scheme 2, the four modified peptides were efficiently converted (51–69 %) into the pyrazole amide derivatives.

Next, we focused on the modification of the p53 activating peptide TSFAEYWALLS.[13] The lineal peptide was assembled on solid phase and modified at the N-terminal Thr residue with methyl tetrazine-NHS ester. The tetrazine-containing peptide reacted in situ with a 5-fold excess of 5-carboxyfluorescein (CFS) and a 10-fold excess of *n*-bNC to afford peptide **15** (Scheme 3a). As observed in Scheme 3d, the CFS-modified peptide gets internalized and

Table 2: MCRs comprising different isonitriles and carboxylic acids.

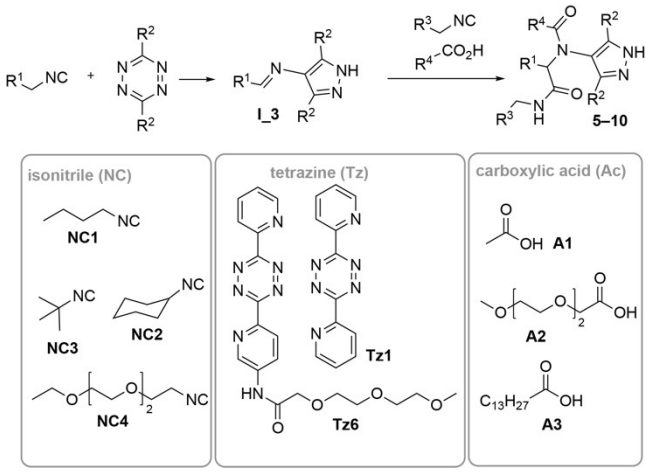

Entry	Product	Tz	NC (step 1/step 2)	Ac	Time	Yield [%]
1	–	**Tz1**	**NC3/NC3**	1	24 h	NP
2	–	**Tz1**	**NC2/NC2**	1	24 h	NP
3	**5**	**Tz1**	**NC1/NC2**	1	110 min	71
4	**6**	**Tz1**	**NC1/NC3**	1	110 min	67
5	**7**	**Tz1**	**NC1/NC1**	2	110 min	24
6	**8**	**Tz1**	**NC1/NC1**	3	90 min	50
7	**9**[a]	**Tz1**	**NC4/NC4**	1	24 h	40
8	**10**[b]	**Tz6**	**NC1/NC1**	1	24 h	50

[a] TFE as solvent. [b] TRIS pH 8.2 as solvent. NP: no MCR product.

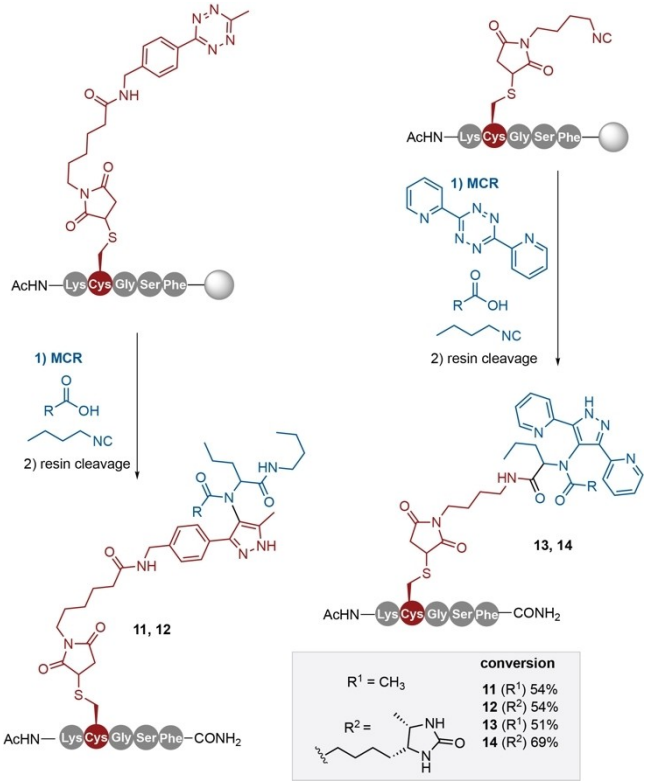

Scheme 2. On-solid phase MCR strategies for the modification of isonitrile- and tetrazine-containing peptides.

colocalizes in vesicles when incubated with HCT-116 cells for 4 h. We next investigated the scope of the reaction for peptide stapling by placing *i*; *i* + 7-spaced Lys and Glu side chains in the above-mentioned sequence (TSFKEYWALLE and TSFEEYWALLK), to be linked through the MCR approach. After the selective removal of the conveniently placed *Allyl* and *Alloc* protecting groups, the Lys side chain was modified using methyl tetrazine-NHS ester, and the peptides reacted overnight with a 10-fold excess of *n*-bNC to afford stapled peptides **16** and **17**. Circular dichroism of two isolated isomers from **16** (Scheme 3c), showed that the stapled peptides have an α-helical secondary structure as reported for other linear and stapled peptides of this family.[14] Peptide **17** was subsequently modified in solution with fluorescein isothiocyanate and further incubated with HCT-116 cells, showing similar internalization and localization patterns to the linear peptide **15** (Scheme 3e).

Owing to the occurrence of the pyrazole ring and its amide derivatives in therapeutics spanning from antipyretic to anticancer applications,[15] we decided to study their cytotoxicity against different cancer cell lines. Compounds **4–6** were assayed against colon SW620, glioblastoma U251, cervix HeLa and breast MDA-MB-231 cancer cell lines. Compound **5** displayed weak cytotoxicity, with IC_{50} values ranging from about 50 to 100 μM (Figure S74). Further, we employed machine learning techniques to evaluate the potential protein targets of pyrazole amide derivatives **1–6**. Random forests were trained on a curated ChEMBL_31 database to predict the normalized activity (pActivity)

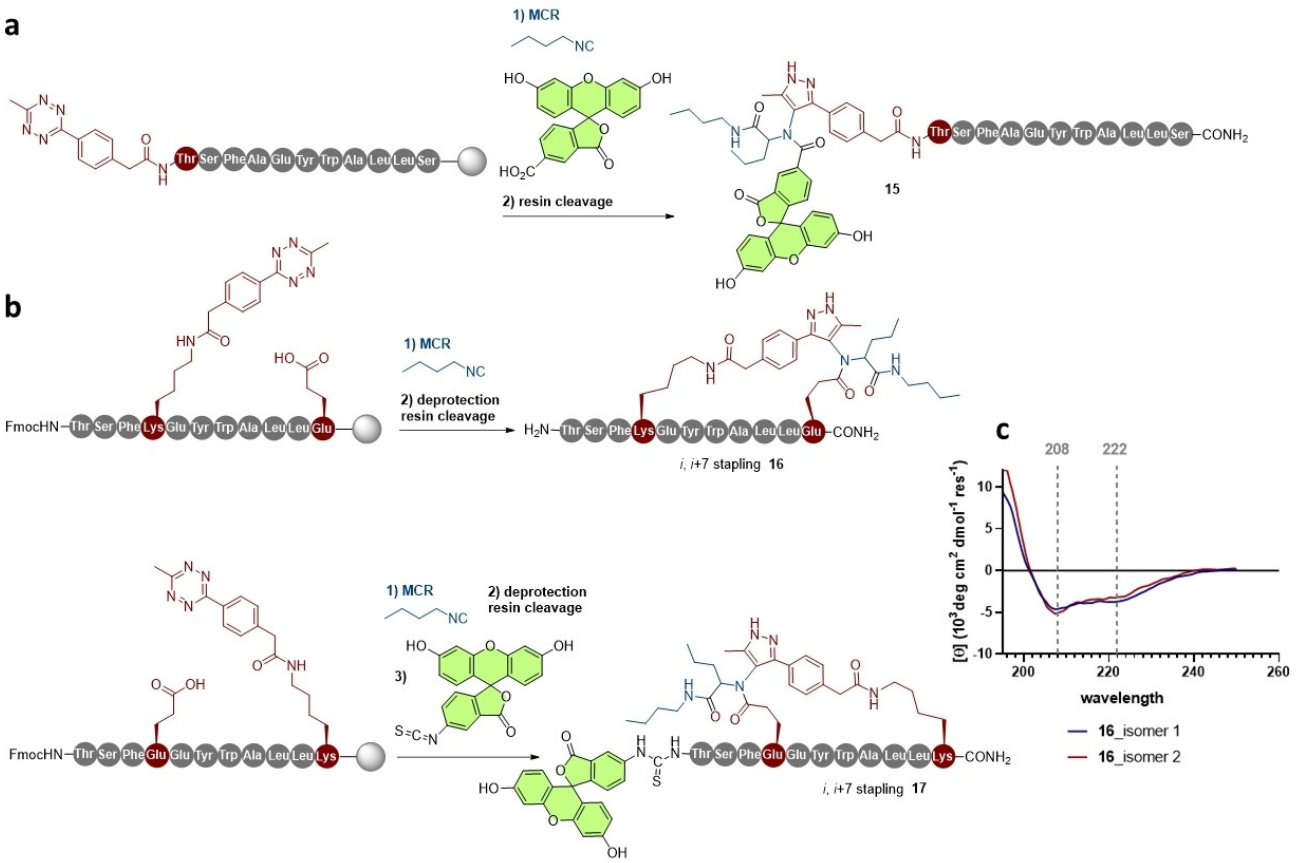

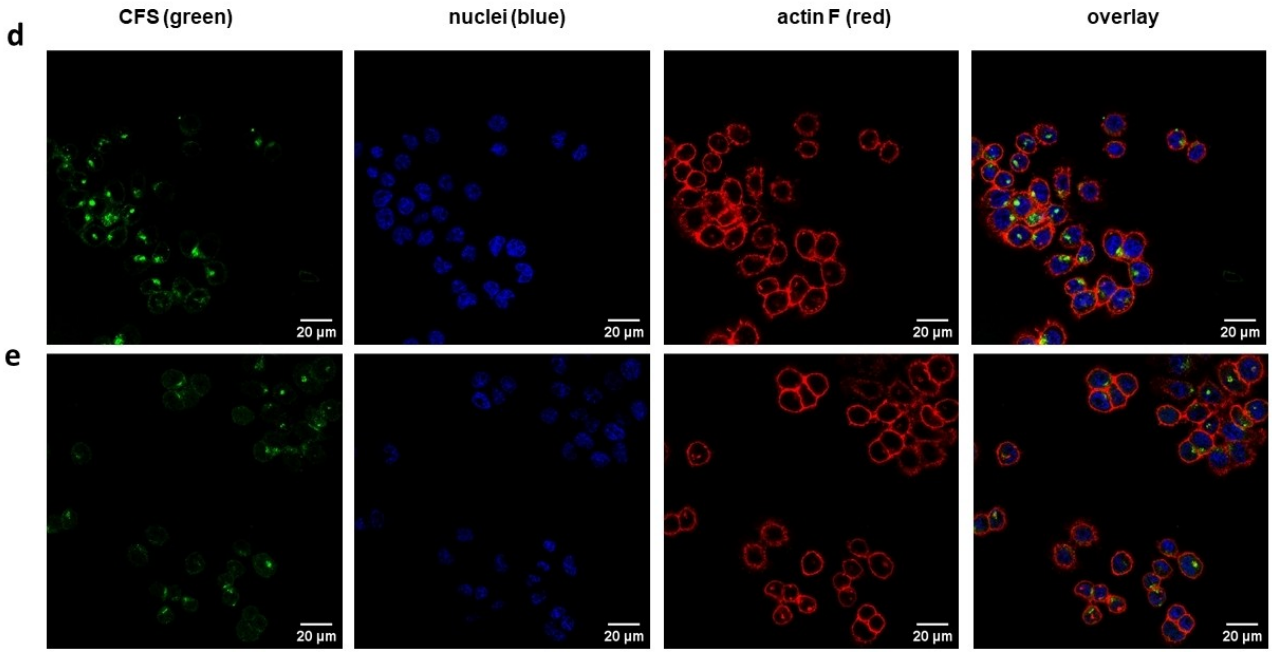

Scheme 3. On-solid-phase MCR strategies for the modification of tetrazine-containing p53 activating peptides. a) Multicomponent modification of an N-terminal tetrazine-containing peptide. b) Two strategies for the multicomponent *i*, *i*+7 stapling of tetrazine-containing peptides. c) Circular dichroism spectra of the two isolated isomers from stapled peptide **16**. d, e) HCT116 cells, seeded at 60000 cells/well were incubated with 20 µM of d) linear peptide **15** and e) FAM-modified stapled peptide **17** for 4.0 h. Cells were imaged using a Leica DMi8 confocal microscope with a 63× oil lens.

against 1171 protein targets. For each target, the hyperparameters were first optimized followed by the activity prediction of the synthesized compounds. Several significative results were found for each compound (pActivity ≥ 5, MAE ≤ 0.5, variance ≤ 1.5, min_pActivity ≤ 4.5, pActivity range > 3, p-value ≤ 0.05). Biological assays were performed for compound **5** since it had the lowest average prediction variance and p-values of significative predictions. OATP1B3 (organic anion transporting polypeptide 1B3) resulted a potential target, with compound **5** presenting moderate inhibition of 38% at 30 μM (Table S7). Also, Tanimoto coefficient analysis yielded a maximum similarity score of 0.24 between compound **5** and the training data, indicating substantial dissimilarity. As such, compound **5** presents a distinct scaffold for OATP1B3 inhibitors, diverging from known inhibitor structures. The overexpression of OATP1B3 in certain cancers highlights the interest of these scaffolds for future drug design for targeted cancer chemotherapy.[16]

To conclude, the unique reactivity of isonitriles allowed the isonitrile-tetrazine (4+1) cycloaddition and the Ugi four-component reaction to be merged into a single MCR process affording stable pyrazole amides. This novel iMCR proved efficient for a broad range of substrates, including solid-phase-immobilized peptides, and showed potential as a late-stage peptide stapling strategy.

Acknowledgements

This work was supported by a Marie Skłodowska-Curie grant (Agreement No. 101018454) from the European Union's Horizon 2020 research and innovation program. We thank the DFG (post-doctoral fellowship, grant no. 493006134, to A.V.V.), Fundação para a Ciência e a Tecnologia (Ph.D. studentship 2022.09827.BD to A.L.D.) and MCIN/AEI/10.13039/501100011033 (PID2021-125946OB-I00 to G.J.O. and CEX2021-001136-S to CIC bioGUNE).

Conflict of Interest

The authors declare no conflict of interest.

Data Availability Statement

The data that support the findings of this study are available in the supplementary material of this article.

Keywords: Chemical Biology · Multicomponent Reactions · Peptides · Tetrazines · Ugi Reaction

[1] a) G. D. P. Gomes, Y. Loginova, S. Z. Vatsadze, I. V. Alabugin, *J. Am. Chem. Soc.* **2018**, *140*, 14272–14288; b) P. Patil, M. Ahmadian-Moghaddam, A. Dömling, *Green Chem.* **2020**, *22*, 6902–6911.
[2] A. Dömling, I. I. Ugi, *Angew. Chem. Int. Ed.* **2000**, *39*, 3168–3210.
[3] M. Passerini, *Gazz. Chim. Ital.* **1921**, *51*, 126.
[4] I. Ugi, *Angew. Chem.* **1959**, *71*, 386.
[5] E. Ruijter, R. Scheffelaar, R. V. Orru, *Angew. Chem. Int. Ed.* **2011**, *50*, 6234–6246.
[6] R. F. Nutt, M. M. Joullie, *J. Am. Chem. Soc.* **1982**, *104*, 5852–5853.
[7] B. Ganem, *Acc. Chem. Res.* **2009**, *42*, 463–472.
[8] P. Imming, R. Mohr, E. Müller, W. Overheu, G. Seitz, *Angew. Chem. Int. Ed.* **1982**, *21*, 284.
[9] J. Tu, M. Xu, S. Parvez, R. T. Peterson, R. M. Franzini, *J. Am. Chem. Soc.* **2018**, *140*, 8410–8414.
[10] H. Stöckmann, A. A. Neves, S. Stairs, K. M. Brindle, F. J. Leeper, *Org. Biomol. Chem.* **2011**, *9*, 7303–7305.
[11] Y. B. Huang, W. Cai, A. Del Rio Flores, F. F. Twigg, W. Zhang, *Anal. Chem.* **2020**, *92*, 599–602.
[12] D. Svatunek, M. Wilkovitsch, L. Hartmann, K. N. Houk, H. Mikula, *J. Am. Chem. Soc.* **2022**, *144*, 8171–8177.
[13] C. J. Brown, S. T. Quah, J. Jong, A. M. Goh, P. C. Chiam, K. H. Khoo, M. L. Choong, M. A. Lee, L. Yurlova, K. Zolghadr, T. L. Joseph, C. S. Verma, D. P. Lane, *ACS Chem. Biol.* **2013**, *8*, 506–512.
[14] M. Pazgier, M. Liu, G. Zou, W. Yuan, C. Li, C. Li, J. Li, J. Monbo, D. Zella, S. G. Tarasov, W. Lu, *Proc. Natl. Acad. Sci. USA* **2009**, *106*, 4665–4670.
[15] M. F. Khan, M. M. Alam, G. Verma, W. Akhtar, M. Akhter, M. Shaquiquzzaman, *Eur. J. Med. Chem.* **2016**, *120*, 170–201.
[16] a) W. Lee, A. Belkhiri, A. C. Lockhart, N. Merchant, H. Glaeser, E. I. Harris, M. K. Washington, E. M. Brunt, A. Zaika, R. B. Kim, W. El-Rifai, *Cancer Res.* **2008**, *68*, 10315–10323; b) M. Muto, T. Onogawa, T. Suzuki, T. Ishida, T. Rikiyama, Y. Katayose, N. Ohuchi, H. Sasano, T. Abe, M. Unno, *Cancer Sci.* **2007**, *98*, 1570–1576; c) F. Silvy, J.-C. Lissitzky, N. Bruneau, N. Zucchini, J.-F. Landrier, D. Lombardo, P. Verrando, *Pigm. Cell Res.* **2013**, *26*, 592–596.

Manuscript received: August 2, 2023
Accepted manuscript online: September 8, 2023
Version of record online: September 20, 2023